JEFF (Fbox11) Genotyping Strategy

Introduction

The Idaho Technology LightScanner is a system used to perform high throughput DNA melting analysis. PCR is performed in the presence of the double stranded DNA binging dye LCGreen. After PCR samples are then heated on the LightScanner and the fluorescence emitted by bound LCGreen is monitored. As the DNA melts the LCGreen is released and so the fluorescence decreases until all the DNA has melted and all LCGreen is unbound. There are several different genotyping methods that can be used on the LightScanner.

Unlabelled probe genotyping is used to distinguish between different homozygote samples at a given SNP where scanning analysis may not have enough sensitivity. Here a 3' blocked oligonucleotide (lunaProbe) is designed that sits directly over the SNP. Asymmetric exhaustive PCR is performed using 5 times the amount of probe and opposite primer. This creates two products, one is the full PCR product between the normal primers and the other is the probe that is bound to the opposite strand.

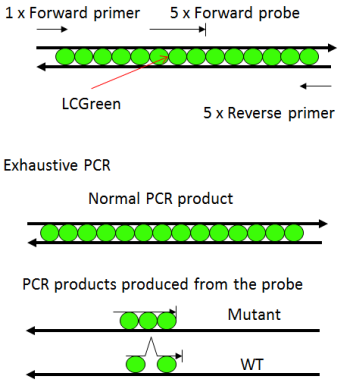

- 3' blocked oligo spanning the SNP (LunaProbe) added to PCR reaction.
- Exhaustive, asymmetric PCR performed with unequal primer concentrations.
- Probe designed to mutant allele. Mutant allele produces the greatest fluorescence.

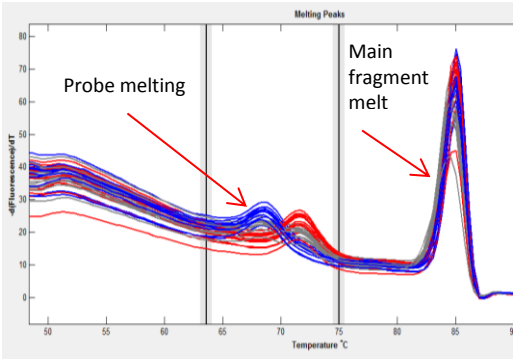

When the products are melted the probe melts at a lower temperature and by focussing analysis on this section hom, het and wt samples can be resolved.

Normalised Melting Curve

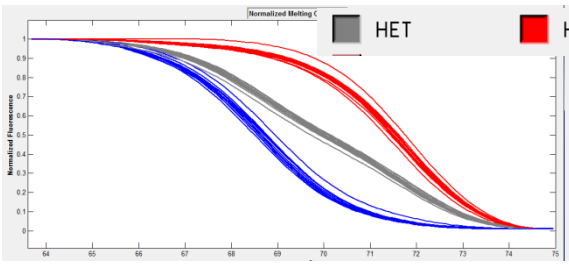

Normalised Melting Peaks

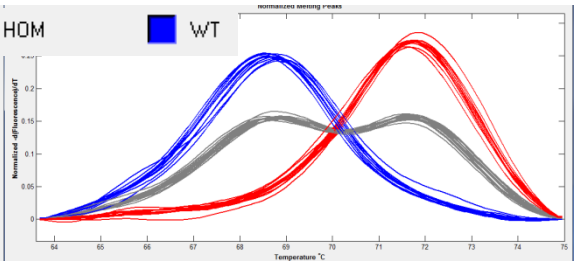

LIGHTSCANNER GENOTYPING

Group:	Deafness
Mutation type:	SNP
Mutant allele:	T
WT allele:	A
Assay Type:	LightScanner LunaProbe
Probe direction:	Reverse

Fragment sequence

ctaatacatgaattgttactattgcctgatgtaaaaattactccacactactaggttctaaacactgactgtaaacgat
atttttaaacagGTAATGCGTTAGCAGGAATTCTGATCAGGACAAACAGTTGTCCTATTGTTCGACATAACAAAATTC
ATGATGGACAGCATGGTGGGATTTATGTGgtaagtgaatgaatgcagttacttaag

Primers/Probe sets 5'>3'

Fbox11Jeff-F	ACACTACTAGGTTCTAAACACTGACT
Fbox11Jeff-R	TAAATCCCACCATGCTGTCCATC
Fbox11Jeff-PR	CTGTTTGTCCTGATCAGAATTCCTGCTA

PCR mix

HotShot master mix	5µl
LCGreen	1µl
Fbox11Jeff-F (20ng/µl)	0.5µl
Fbox11Jeff-R (20ng/µl)	0.1µl
Fbox11Jeff-PR (20ng/µl)	0.5µl
DNA (1/10 dil ABI)	2µl
ddH2O	0.9µl

PCR program

LSGENO60H (annealing temperature 60 °C with hybridisation step)

Control method	Calculated
Lid control mode	Off (no need for heated lid as sample is overlaid with oil)
Lid pressure	Microplate

1) 95°C for 2 min
2) 95 °C for 30 sec — PCR cycle
3) 60 °C for 30 sec
4) 72 °C for 30 sec
5) Cycle, step 2 55 times
6) 95 °C for 30 sec — Hybridisation
7) 25 °C for 30 sec
8) 15 °C for 30 sec

Example

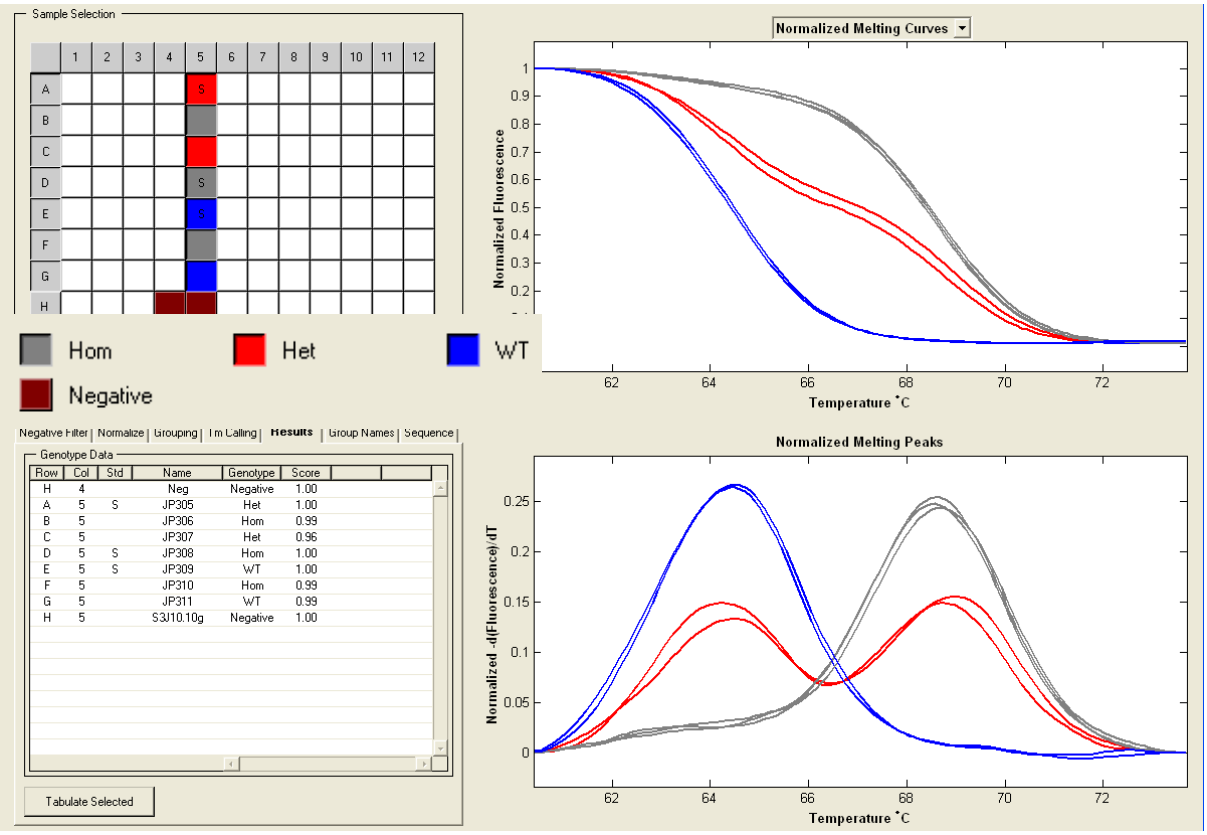
Sample Selection
Hom
Het
WT
Negative
Normalized Melting Curves
Normalized Fluorescence
Temperature °C
Negative Filter | Normalize | Grouping | Tm Calling | Results | Group Names | Sequence
Genotype Data
Row Col Std Name Genotype Score
H 4 Neg Negative 1.00
A 5 S JP305 Het 1.00
B 5 JP306 Hom 0.99
C 5 JP307 Het 0.96
D 5 S JP308 Hom 1.00
E 5 S JP309 WT 1.00
F 5 JP310 Hom 0.99
G 5 JP311 WT 0.99
H 5 S3J10.10g Negative 1.00
Tabulate Selected
Normalized Melting Peaks
Normalized -d(Fluorescence)/dT
Temperature °C

Human Molecular Genetics, 2006, Vol. 15, No. 22 ***3273–3279***
doi:10.1093/hmg/ddl403
Advance Access published on October 11, 2006

A mutation in the F-box gene, *Fbxo11*, causes otitis media in the *Jeff* mouse

Rachel E. Hardisty-Hughes[1], Hilda Tateossian[1], Susan A. Morse[1], M. Rosario Romero[1], Alice Middleton[1], Zuzanna Tymowska-Lalanne[1], A. Jackie Hunter[2], Michael Cheeseman[1,3] and Steve D.M. Brown[1,*]

[1]MRC Mammalian Genetics Unit, Harwell, OX11 0RD, UK, [2]GlaxoSmithKline Pharmaceuticals, New Frontiers Science Park, Harlow CM19 5AW, UK and [3]MRC Mary Lyon Centre, Harwell, OX11 0RD, UK

Received July 10, 2006; Revised and Accepted September 21, 2006

Otitis media (OM), inflammation of the middle ear, is the most common cause of hearing impairment and surgery in children. Recurrent and chronic forms of OM are known to have a strong genetic component, but nothing is known of the underlying genes involved in the human population. We have previously identified a novel semi-dominant mouse mutant, *Jeff*, in which the heterozygotes develop chronic suppurative OM (Hardisty, R.E., Erven, A., Logan, K., Morse, S., Guionaud, S., Sancho-Oliver, S., Hunter, A.J., Brown, S.D. and Steel, K.P. (2003) The deaf mouse mutant Jeff (Jf) is a single gene model of otitis media. J. Assoc. Res. Otolaryngol., 4, 130–138.) and represent a model for chronic forms of OM in humans. We demonstrate here that *Jeff* carries a mutation in an F-box gene, *Fbxo11*. *Fbxo11* is expressed in epithelial cells of the middle ears from late embryonic stages through to day 13 of postnatal life. In contrast to *Jeff* heterozygotes, *Jeff* homozygotes show cleft palate, facial clefting and perinatal lethality. We have also isolated and characterized an additional hypomorphic mutant allele, *Mutt*. *Mutt* heterozygotes do not develop OM but *Mutt* homozygotes also show facial clefting and cleft palate abnormalities. FBXO11 is one of the first molecules to be identified, contributing to the genetic aetiology of OM. In addition, the recessive effects of mutant alleles of *Fbxo11* identify the gene as an important candidate for cleft palate studies in the human population.

INTRODUCTION

Otitis media (OM), inflammation of the middle ear, is the most common cause of hearing impairment in children (1,2). In addition, it remains the commonest cause of surgery in children in the developed world. Acute episodes of OM are usually associated with middle ear infections by the bacterial pathogens *Streptococcus pneumoniae* and *Haemophilus influenzae* (3). However, prolonged stimulation of the inflammatory response accompanied by poor mucociliary response can lead to a persistent middle ear effusion (OME), and in many children, recurrent or chronic suppurative forms of the disease may develop. The prevalence of OM along with its recurrent and chronic nature underlies the frequency of tympanostomies undertaken in the affected children.

There is a variety of evidence suggesting a number of risk factors that predispose to the development of recurrent and chronic forms of OM, including poor mucociliary clearance, craniofacial abnormalities and the presence of an inflammatory stimulus, such as bacteria. However, evidence from studies in the human population and in mouse models demonstrates that there is a very significant genetic component predisposing to recurrent and chronic forms of OM (4–7). OM is a multifactorial disease and the underlying genetic determinants are likely to be complex (8). Several studies have focussed on studying human candidate genes and the association of polymorphisms with OM susceptibility (9). Although several inbred strains are predisposed to the development of OM, the genetic analysis of these strains is compounded by the complex genetic bases and the low penetrance of the phenotype. Moreover, there are a number of mouse mutants that demonstrate OM as part of a more complex syndrome with a wide spectrum of phenotypes. Our approach to identifying genes that are involved in the OM susceptibility has been to study highly penetrant mouse mutants that demonstrate OM in the absence of other diverse pathology and represent

*To whom correspondence should be addressed: s.brown@har.mrc.ac.uk

appropriate models for OM in the human population. These represent start points to uncover the genetic pathways involved in OM and as candidate genes for human association studies.

The *Jeff* mouse mutant was identified from a deafness screen as part of a large-scale ENU mouse mutagenesis programme (10). *Jeff* is a dominant mutant that in heterozygotes displays a conductive deafness due to the development of a chronic suppurative OM that develops at weaning and is associated with raised thresholds for a cochlear nerve response (4). *Jeff* heterozygotes are smaller than their wild-type littermates and have a mild craniofacial abnormality. In older *Jeff* heterozygote mice, hearing thresholds are raised beyond what might be expected of a simple conductive hearing impairment. Indeed, endocochlear potentials in these mice were abnormally low, suggesting that the mutation in older mice is associated with sensorineural hearing loss due to impaired strial function. There are many reports of middle ear disease in humans associated with a sensorineural component to the hearing loss. Overall, the disease pathology observed in *Jeff* indicates that the mutant is an appropriate model for OM in humans.

We have proceeded to identify the gene underlying the *Jeff* mutant. *Jeff* carries a mutation in the F-box gene, *Fbxo11*. In addition, we have isolated and characterized an additional ENU mutant allele at this locus, the *Mutt* mutation. Both *Jeff* and *Mutt* homozygotes demonstrate cleft palate defects, facial clefting and perinatal lethality. *Fbxo11* represents an important candidate gene for the study of the genetic pathways involved in OM in the human population. In addition, the role of *Fbxo11* in the development of the palatal shelves implicates that this as an important candidate for studies of cleft palate in the human population.

RESULTS

Mapping and identification of the *Jeff* mutation

The *Jeff* mutant is a semi-dominant mutation with the heterozygote previously described as having chronic proliferative OM (4). The *Jeff* mutation was mapped using backcrosses to an ~300 kb region of distal chromosome 17 flanked by the markers *SNPMGUC17* and *D17Mit1* (see Materials and Methods) (data not shown). On the basis of Ensembl predictions (http://www.ensembl.org), this region contains three genes and two pseudogenes. The three genes in the region are *Fbxo11*, *Msh6* and a novel transcript, the 40S ribosomal *s24* gene.

In order to identify the *Jeff* mutation, we carried out both denaturing high-performance liquid chromatography (DHPLC) screens and sequence analysis of all three genes, *Fbxo11*, *Msh6* and *s24*. Ultimately, we sequenced all coding regions. This analysis revealed only one coding change in exon 13 of *Fbxo11* (Fig. 1A), an A–T transversion at base 1472 causing a non-conservative glutamine to leucine change at amino acid 491. The change occurs in a highly conserved region of this protein that has been maintained through evolution (Fig. 1C). The *Fbxo11* locus has one predicted transcript and encodes a protein of 850 amino acids, coded for by 22 exons. The 94 kDa protein consists of two carbohydrate-binding domains, an F-box motif and a zinc-finger domain (Fig. 1A).

Characterization of the *Jeff* homozygous mutant phenotype

The mapping of the *Jeff* mutation allowed us to genotype and examine mice homozygous for the *Jeff* mutation. One hundred percent of *Jeff* homozygotes demonstrated perinatal lethality, dying at birth or within a few hours ($n = 36$) due to respiratory problems (gasping for air and with air in their stomach). Homozygotes are born with upper eyelids open and show clefting of the hard or soft palate as well as facial clefting (Fig. 2B).

The original description of the OM phenotype in adult *Jeff* heterozygotes (4) was based on sagittal sections of bisected heads and this is not optimal to evaluate the possibility of cleft palate. In view of the finding of cleft palate in *Jeff* homozygous mice, the palate of *Jeff* heterozygotes was examined in coronal sections of the snout in a series of 17 *Jf*/+ mice 5, 13, 28, 56 and 120 DAB (days after birth). None had cleft palate and OM was clearly evident by 28 DAB onwards.

An additional *Fbxo11* mutant allele: *Mutt*

We used DNA and sperm archives derived from ENU mutagenesis programmes (11) to identify an additional allele at the *Fbxo11* locus. We screened the first seven exons of *Fbxo11* employing heteroduplex analysis of 4200 mutant mice and identified a further point mutation in exon 7, leading to a non-conservative serine to leucine change, S244L (Fig. 1A) in a conserved region of the protein (Fig. 1B). We rederived this second allele of *Fbxo11*, *Mutt*, and examined the heterozygous and homozygous phenotype.

At 48 DAB a proportion of *Mutt* heterozygotes (13%, $n = 128$) showed a reduced startle response to a toneburst of ~24 kHz, 90 dB SPL and a mild craniofacial abnormality, a shortened face (57%), similar to the craniofacial phenotype of the *Jeff* heterozygote (4) but did not have OM at 39–45 DAB (0/63 examined), suggesting that *Mutt* is a weaker hypomorphic allele of *Fbxo11* in comparison to the *Jeff* mutation. However, similar to the *Jeff* mutation, we found that a small proportion of *Mutt* homozygotes (17%, $n = 52$) showed perinatal lethality with these mice, demonstrating mild clefting of the palate along with facial clefting in some instances (Fig. 2D, 2 g). The small proportion of *Mutt* homozygotes demonstrating perinatal lethality, in comparison to the 100% lethality found in *Jeff* homozygotes, also indicates the hypomorphic nature of the *Mutt* allele. The surviving *Mutt* homozygotes demonstrated a marked craniofacial abnormality—short face (84%) and reduced hearing (42%)—using the 24 kHz, 90 dB SPL toneburst but did not have OM (0/17 examined).

Compound heterozygotes carrying both *Jeff* and *Mutt* alleles showed a similar phenotype to *Jeff*. About 88% of *Jeff/Mutt* mice ($n = 19$) survived and demonstrated a shortened face, reduced hearing (in response to a click box) and OM. Thus, most of the compound heterozygotes recapitulated the *Jeff* heterozygous phenotype again indicating the hypomorphic nature of the *Mutt* mutation. However, importantly, a small

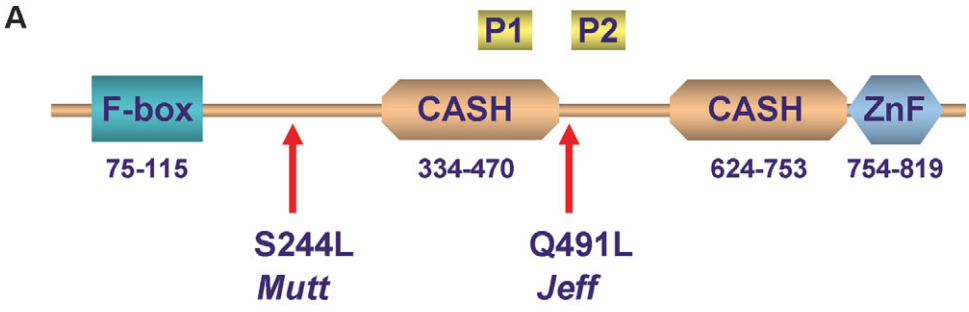

B

H. sapiens	IENTRDSTFVFMEG
M. musculus	IENTRDSTFVFMEG
Mutt Fbxo11	IENTRDLTFVFMEG
R. norvegicus	IENTRDSTFVFMEG
G. gallus	IENTRDSTFVFMEG
D. rerio	IENTRDSTFVFMEG
F. rubipes	IENTRDSTFVFMEG
D. melanogaster	LEREAGSTVMFVEG
A. gambiae	LERESESTVMFVEG
C. elegans	LEGSKNTALTFTDG
C. intestinalis	IENMCETTIVFTEG

C

H. sapiens	NALAGIQIRTNSCP
M. musculus	NALAGIQIRTNSCP
Jeff Fbxo11	NALAGILIRTNSCP
R. norvegicus	NALAGIQIRTNSCP
G. gallus	NALAGIQIRTNSCP
D. rerio	NALAGIQIRTNSCP
F. rubipes	NALAGIQIRTNSCP
D. melanogaster	NALAGIQIRSQSDP
A. gambiae	NALAGIQIRTTSDP
C. elegans	NALAGIQIRTNSDP
C. intestinalis	NALAGIQIRTNSSP

Figure 1. Mutations in the Fbox gene, ***Fbxo11***. (**A**) Protein structure of *Fbxo11* from sequence predictions. The molecule consists of an F-box motif, two carbohydrate-binding (CASH) domains and a zinc finger domain (ZnF). The amino acid numbers constituting these domains are shown below the appropriate domain. The positions of the *Jeff* and *Mutt* mutations are also indicated (arrows). The position of peptides, flanking the *Jeff* mutation, used to raise a polyclonal antibody CIYVHEKGRGQFIEN (P1) and CPIVRHNKIHDGQHG (P2) is indicated (see also Materials and Methods). (**B**) Sequence lineups of the amino acids 238–251 (in the mouse) in different species. Note the change S–L in *Mutt* DNA (shown in red). (**C**) Sequence lineups of the amino acids 485–498 (in the mouse) in different species. Note the change Q–L in *Jeff* DNA (shown in red).

proportion (12%, $n = 19$) of the compound heterozygotes demonstrated facial clefting (Fig.2E) and failed to survive, similar to *Jeff* homozygotes and a proportion of the *Mutt* homozygotes (discussed earlier).

Expression of *Fbxo11* during mouse development

Peptides flanking the *Jeff* mutation were used to raise an antibody to FBXO11 (Fig. 1A). Immunohistochemistry on paraffin sections was performed to study the expression of FBXO11 in wild-type embryonic tissue (from E8.5 to E18.5), in newborn, 4 DAB, 13 DAB and 21 DAB head tissue and in various adult tissues. At E8.5, we detected no labelling. At E9.5 and E10.5 (Fig. 3A), FBXO11 signal was restricted to the developing heart tissue. By E11.5 and E12.5, labelling was observed in the liver (Fig. 3B) that subsequently extended to the muscle by E13.5. By E14.5, labelling is still detected in the heart, liver and muscle, but signal is now seen in the developing secondary palate including the nasal, medial and oral epithelia of the palatal shelves, as they elevate above the tongue (Fig. 3C). At E15.5 and E16.5, the lung, kidney, heart, liver, muscle and adrenal gland are all labelled. At this time, fusion of the palate shelves has occurred, with signal confined to the nasal and oral epithelia. By E17.5, signal in the lung is confined to the bronchial epithelial cells (Fig. 3D) and expression is evident in the bone marrow, skin, tissue macrophages, osteoblasts, kidney, liver and spleen. At E18.5, bone marrow, liver, kidney and muscle are positive, but signal in heart and lung is beginning to fade out. At this time, labelling is first detected in the middle ear epithelium (Fig. 3E). At the new born stage, labelling is strong in the middle ear and confined to the mucin secreting cells, as well as persisting in bone marrow (Fig. 3F), kidney and liver. Middle ear expression persists in postnatal head tissue at 4 DAB (Fig. 3 g) and 13 DAB (Fig. 3 h) and has declined by 21 DAB (data not shown). Expression of FBXO11 therefore occurs in the middle ear just preceding the period OM is evident in mice. In adult, tissue expression is seen in the alveolar macrophages of the lung, the glomeruli and the collecting tubules of the kidney, the midbrain, the heart and the muscle (data not shown).

DISCUSSION

The *Jeff* mouse mutant is a model of chronic OM in the human population. We have therefore proceeded to map and identify the mutation underlying the *Jeff* mutant. The *Jeff* mutant carries a mutation in the F-box protein, *Fbxo11*. FBXO11 is

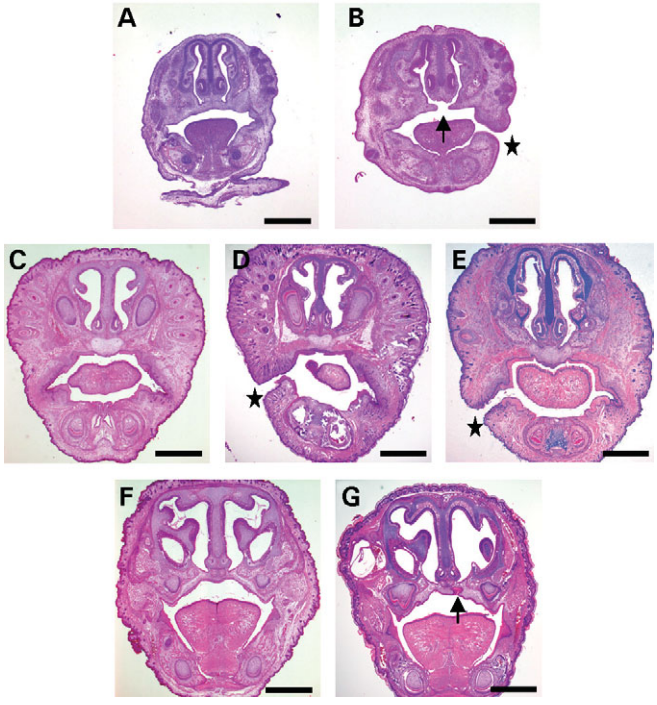

Figure 2. Coronal sections of the head (H&E staining) demonstrating the palate and facial phenotypes of late embryonic *Jeff* homozygotes and perinatal *Mutt* homozygotes and *Jeff/Mutt* compound heterozygotes that fail to thrive. Scale bar: 1 mM. Facial clefts are marked with a star and cleft palate is marked with an arrow. (**A**) E15.5 wild-type; (**B**) E15.5 *Jeff* homozygote with facial cleft and cleft palate; (**C**) 5 DAB wild-type, rostral section; (**D**) 5 DAB *Mutt* homozygote with facial cleft, rostral section; (**E**) 1 DAB compound *Jeff/Mutt* heterozygote with facial cleft, rostral section; (**F**) 5 DAB wild-type, caudal section; (**G**) 5 DAB *Mutt* homozygote with mild cleft palate, caudal section.

expressed in the middle ear epithelium just preceding the period OM is evident in the *Jeff* mouse. We have also isolated and characterized an additional mutant allele at the *Fbxo11* locus, the *Mutt* mutation. The *Mutt* allele does not develop OM, suggesting it is a hypomorphic allele at the *Fbxo11* locus. However, like the *Jeff* mutation, a proportion of *Mutt* homozygotes show facial clefting and cleft palate. At E14.5, FBXO11 is expressed in the margins of the palatal shelves. The mutational and expression analysis of the *Fbxo11* gene identifies a new locus involved with cleft palate and facial clefts in the mouse (12–15). It will be important to investigate the contribution of this F-box protein and its substrate to cleft palate defects in the human population.

Fbxo11 is one member of a large family of proteins involved with ubiquitination. Much of the targeted protein ubiquitination that occurs in eukaryotic organisms is performed by cullin-based E3 ubiquitin ligases, which form a superfamily of modular E3s (16). The best understood cullin-based E3 is the SCF ubiquitin ligase (17–19) composed of a modular E3 core, containing CUL1 and RBX1, SKP1 and a member of the F-box family of proteins (20–25). The interaction of the F-box protein with SKP1 occurs via the F-box motif, an approximately 40 amino acid motif first identified in yeast and human cyclin-F. F-box proteins also contain further interaction domains that bind ubiquitination targets. A recent study (16) identified 74 mouse genes encoding recognizable F-box motifs subdivided into three subsets: FBXL (containing leucine rich repeats), FBXW (containing WD40 motifs) and FBXO (proteins that contain an F-box and an 'other' identifiable motif) of which there are 47 members to date (16,26). A fragment of FBXO11 was originally identified in a differential expression analysis of cultured melanocytes from generalized vitiligo patients versus control cells (27). This cDNA which they called VIT1 was found to be absent in melanocytes from vitiligo patients. Recently, FBXO11/PRMT9 was identified as an arginine methyltransferase with a structure different from all other known protein arginine methyltransferases (28), but a potentially diverse set of targets (29).

Very little is known of the function of most F-box proteins in disease and development but there are examples of proteins from all three subclasses playing pivotal roles. It is interesting to surmise, however, on the role that ubiqutination and protein turnover might play in regulating signalling networks involved in epithelial inflammatory events in the middle ear and the involvement of FBXO11. Nontypeable *H. influenzae* (NTHi) is often associated with middle ear infections and acute episodes of OM. NTHi activates an intricate array of host epithelial signalling networks (30) that contribute to the pathogenesis of the disease. One signalling pathway, by example, leads to the activation of NF-κB and up-regulation of cytokines IL-1β, IL-8, TNFα as well as the mucin, MUC2. NF-κB pathways are the sites of several control points involving ubquitination (31). For example, NF-κB is maintained in an inactive state by binding to the protein IκB. Following phosphorylation of IκB, IκB is targeted for ubiquitination and degradation by the proteosome, thus freeing NF-κB for entry into the nucleus (32). It will be important to identify the protein substrates of FBXO11 that are targeted for ubiquitination and to identify whether they impact on the known signalling pathways that are involved in epithelial inflammatory responses in the middle ear.

The characterization of *Fbxo11* as a major gene involved in susceptibility to OM identifies a further function for this class of proteins. In addition, it provides an important locus for candidate gene studies in the human population. Indeed, it is noteworthy that our initial studies of *FBXO11* SNPs in human OM families have uncovered nominal evidence of association, indicating the genetic involvement of human *FBXO11* in chronic OM with effusion and recurrent OM (33).

MATERIALS AND METHODS

Mice and husbandry

Mice were housed in conventional cages and were provided with food and water *ad libitum* and maintained according to home office and ethical regulations. Sentinel health screening from this old MRC Harwell mouse house showed the presence of the following FELASA listed agents (http://www.felasa.org) (34): MHV (judged by histology to be enteropathic strains), Adenovirus II and TMEV, none of which is primary respiratory pathogens. Intestinal flagellates, pinworms and the opportunist respiratory pathogen *Pasteurella pneumotropica* were also common isolates. Non-FELASA listed bacteria isolated from the nasopharynx of sentinel mice included

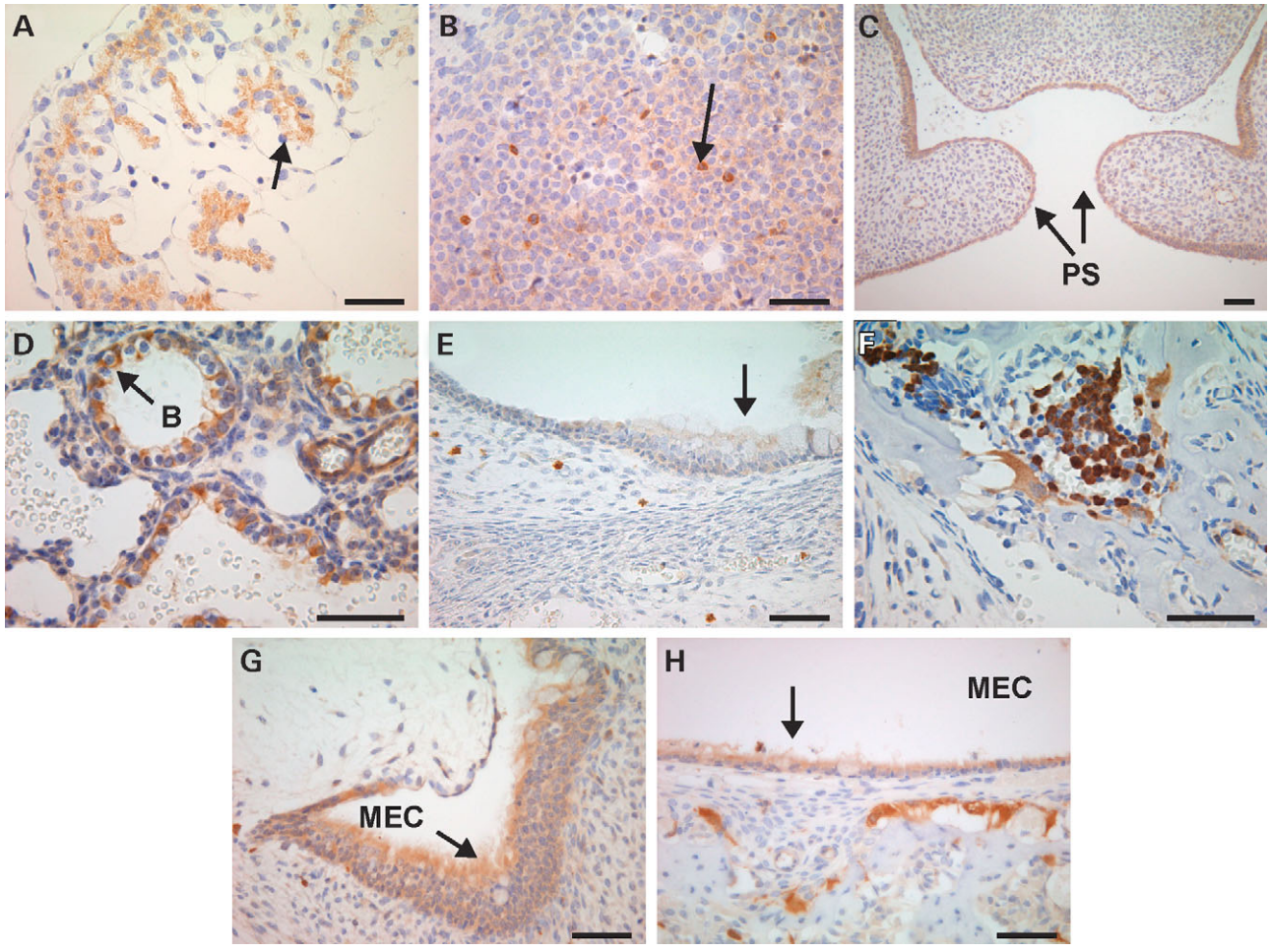

Figure 3. Expression of FBXO11 in wild-type tissues at various developmental and adult stages of the mouse. Scale bar: 50 μm. (**A**) E10.5 heart tissue expression, is in developing cardiac cells (arrow); (**B**) E11.5 liver tissue, expression is in haematopoietic cells (arrow); (**C**) E14.5 palate, expression is in the margins of the palatal shelves (PS) (arrows); (**D**) E17.5, bronchial epithelial cells (arrow): B, bronchiole; (**E**) E18.5, middle ear epithelial cells (arrow); (**F**) new-born stage, bone marrow; (**G**) 4 DAB, middle ear epithelium (arrow); (**H**) 13 DAB, middle ear epithelium (arrow). MEC, middle ear cavity.

Staphylococcus spp., *Staphylococcus aureus*, Alpha-haemolytic streptococci and other *Streptococcus* spp. (but not *S. pneumoniae*). The *Jeff* colony has subsequently been rederived by embryo transfer into a new MRC Harwell SPF facility, the Mary Lyon Centre, and is maintained on the C57BL/6J background. The stocks are free of FELASA listed agents, but the nasopharynx of sentinel mice has similar non-FELASA list streptococcal and staphylococcal flora.

Genetic mapping

ENU mutagenesis was carried out on a BALB/c background and males outcrossed to C3H/HeN (10). For inheritance testing, affected F1 individuals were backcrossed to C3H/HeN. We originally mapped the *Jeff* mutation to chromosome 17, based on 30 affected individuals (4). To further increase the resolution of this genetic map, 920 meioses were generated. Mapping was further enhanced by a second backcross [(*Jf*/+ × C57BL/6J) × (C57BL/6J)]. Markers and primer sequences are available on request from the authors.

Denaturing high-performance liquid chromatography

Mutation detection was performed using a transgenomic wave machine, utilizing DHPLC. The system was run according to manufacturer's instructions (Transgenomic). Exons to be screened were amplified using primers placed in flanking introns. DNAs from a *Jf*/+ mouse and a BALB/c (+/+) mouse were amplified for each exon using *Taq* polymerase (ABgene), at an annealing temperature of 55°C. Following amplification, heteroduplexes were formed by thermocycling.

Sequencing

PCR products from *Jf*/+ and BALB/c DNA were purified using QIAquick PCR purification kit (Qiagen). Direct sequencing was performed using Applied Biosystem's Bigdye Terminator v3.1 cycle sequencing mix and sequenced on an ABI prism 377 DNA sequencer according to manufacturer's instructions.

Genotyping

Genotyping for *Jeff* mice was performed by PCR amplification of the exon containing the mutation followed by digest with BclI. Amplification of exon 13 using primers 5′-TGC CTG ATG TAA AAA TTA CTC CAC-3′ and 5′-TCT CTA GGG ATC AGG CAC ATC-3′ yields a product of 199 bp. In the presence of the mutation, a *Bcl*I restriction site is introduced giving two bands of 132 and 67 bp.

To genotype *Mutt* mice, genomic DNA was used to PCR amplify the region containing the mutation with primers 5-′ biotin TTC AGA GCC TTC CAT GAA CAC G-3′ and 5′-NNN CCT GGC AAG GTT GCA GAC-AA-3′. The PCR product (77 bp) and primer 5′-TCA TCA TTG AGA ACA CTA GA-3′ were used for subsequent pyrosequencing SNP analysis to identify differences in sequences.

Fbxo11 polyclonal antibody

A polyclonal antibody against mouse FBXO11 was produced by Covalab UK (www.covalab.com) using two peptides as antigens. The peptide sequences were 419CIYVHEKGRGQ-FIEN433 and 497CPIVRHNKIHDGQHG511 and they lay in the central unique part of the mouse Fbxo11 protein. Both peptides were injected together into rabbits. The serum from the immunized animals was collected and the antibody was purified by affinity chromatography using the peptides. Affinity-purified antibody was tested on western blot using whole mouse head lysates where it recognizes bands of ∼46, 32 and 26 kDa. Various cell lines showed bands of similar sizes by western blot. Since the antibody does not detect full-length protein, we tested its specificity in various ways. First, pre-incubation of the affinity-purified antibody with increasing amounts of the peptides used as antigens for its production gradually abolished the signal detected by western blot and immunohistochemistry. Secondly, following immunoprecipitation with the purified antibody, the 46 kDa band was digested with trypsin and identified as FBXO11 by peptide mass fingerprint (data not shown). In addition, we transfected Cos-7 cells with a plasmid containing the mouse FBXO11 sequence tagged to the Xpress epitope (Invitrogen). In lysates from transfected Cos-7 cells, anti-Fbxo11 polyclonal antibody recognizes an identical band to that detected by anti-Xpress antibody and of the expected size (∼94 kDa).

Western blotting

Mouse head tissue was homogenized at 4°C in lysis buffer (50 mM HEPES, pH 7.4, 10% Triton X-100, 50 mM sodium phosphate, 10 mM EDTA, 10 mM sodium fluoride, 10 mM sodium orthovanadate, 2 mM benzamidine and a protease inhibitor cocktail). Homogenate was solubilized on ice for 1 h and centrifuged at 4°C, first at 3000 rpm for 15 min and then at 14 000 for 1 h at 4°C. The supernatant was run in a 4–12% acrylamide gel (Invitrogen NuPAGE) and then the gel was blotted onto a PVDF membrane. The membrane was incubated in a blocking solution containing PBS, 0.1% Tween-20 and -5% skimmed milk for 1 h at room temperature. After blocking, the membrane was incubated with anti-Fbxo11 antibody at 7.5 μg/ml in blocking solution for 1 h at room temperature. After four washes in PBS/0.1% Tween-20, the membrane was incubated with anti-rabbit IgG conjugated to HRP for 1 h at room temperature and washed as before. The bands labelled by the antibody were detected by ECL-Plus (GE Healthcare).

Histology

Whole embryos (E8.5–E18.5), new born mice, adult heads (4, 13 and 21 DAB) and various adult tissues were fixed in 10% buffered formaldehyde, decalcified in EDTA (embryos E14.5–18.5 for 3–5 days and adult heads for 4 weeks) and embedded in paraffin. Four-micrometer-thick transverse and coronal sections were obtained, de-paraffinized in xylene substitute and rehydrated via a graded ethanol solutions. For morphological observations, sections were stained with H&E. The ears of 39–45 DAB *Mutt* mice on the C3H/HeN background (+/+ $n = 17$, *Mutt*/+ $n = 63$, *Mutt*/*Mutt* $n = 17$) and double heterozygotes (*Jf*/*Mutt* $n = 17$) were surveyed for OM. The ears and palates were surveyed in SPF *Jeff* heterozygotes on C57BL/6J background (two 5 DAB, two 13 DAB, three 28 DAB, five 56 DAB, five 120 DAB). These heads were decalcified 24–48 h with Immunocal (Decal Corp. Tallman, NY, USA) and stained with H&E.

Immunostaining

For immunohistochemical analysis, the avidin–biotin complex (ABC) method was used. Endogenous peroxidase activity was quenched with 3% hydrogen peroxide in isopropanol for 20 min. The slides were pre-treated by boiling in a microwave in 1 mM EDTA, pH 8, for E8.5–13.5 embryos and in water, for E14.5–18.5 embryos and all adult tissues, for 14 min, cooled at RT for 20 min and rinsed with phosphate-buffered saline. The immunostaining was performed using a DAKO autostainer at room temperature. To inhibit non-specific endogenous biotin staining, the DAKO Biotin Blocking System was used (DAKO, X0590). A blocking solution of 10% swine serum (DAKO, X0901) was used for 1 h. Fbxo11 antibody incubations were conducted for 1 h using a 1:200 dilution. Biotinylated swine anti-rabbit antibody (DAKO, E0353) and ChemMate Detection Kit (DAKO, K5001) were used to develop the specific signals. Negative control sections were stained with the FBXO11 antibody previously incubated with the blocking peptides and processed identically. The slides were counterstained with haematoxylin.

ACKNOWLEDGEMENTS

This work was funded by the MRC and by the European Commission under contract number QLG2-CT-2002-00930. The authors would like to thank Caroline Barker, Adele Seymour, Jennifer Corrigan and Terry Hacker for histology services.

Conflict of Interest statement. None declared.

REFERENCES

1. Davidson, J., Hyde, M.L. and Alberti, P.W. (1989) Epidemiologic parameters in childhood hearing loss: a review. *Int. J. Pediatr. Otorhinolaryngol.*, **17**, 239–266.
2. Kubba, H., Pearson, J.P. and Birchall, J.P. (2000) The aetiology of otitis media with effusion, a review. *Clin. Otolaryngol.*, **25**, 181–194.
3. Bluestone, C.D. and Klein, J.O. (2001) *Otitis Media on Infants and Children*. W.B. Saunders Company.
4. Hardisty, R.E., Erven, A., Logan, K., Morse, S., Guionaud, S., Sancho-Oliver, S., Hunter, A.J., Brown, S.D. and Steel, K.P. (2003) The deaf mouse mutant Jeff (Jf) is a single gene model of otitis media. *J. Assoc. Res. Otolaryngol.*, **4**, 130–138.
5. Kvaerner, K.J., Tambs, K., Harris, J.R. and Magnus, P. (1997) Distribution and heritability of recurrent ear infections. *Ann. Otol. Rhinol. Laryngol.*, **106**, 624–632.
6. Casselbrant, M.L., Mandel, E.M., Fall, P.A., Rockette, H.E., Kurs-Lasky, M., Bluestone, C.D. and Ferrell, R.E. (1999) The heritability of otitis media: a twin and triplet study. *JAMA*, **282**, 2125–2130.
7. Daly, K.A., Brown, W.M., Segade, F., Bowden, D.W., Keats, B.J., Lindgren, B.R., Levine, S.C. and Rich, S.S. (2004) Chronic and recurrent otitis media: a genome scan for susceptibility loci. *Am. J. Hum. Genet.*, **75**, 988–997.
8. Zheng, Q.Y., Hardisty-Hughes, R. and Brown, S.D.M. (2006) Mouse models as a tool to unravel the genetic bases for human otitis media. *Brain Res*, **1091**, 9–15.
9. Casselbrant, M.L. and Mandel, E.M. (2005) Genetic susceptibility to otitis media. *Curr. Opin. Allergy Clin. Immunol.*, **5**, 1–4.
10. Nolan, P.M., Peters, J., Strivens, M., Rogers, D., Hagan, J., Spurr, N., Gray, I.C., Vizor, L., Brooker, D., Whitehill, E. *et al*. (2000) A systematic, genome-wide, phenotype-driven mutagenesis programme for gene function studies in the mouse. *Nat. Genet.*, **25**, 440–443.
11. Quwailid, M.M., Hugill, A., Dear, N., Vizor, L., Wells, S., Horner, E., Fuller, S., Weedon, J., McMath, H., Woodman, P. *et al*. (2004) A gene-driven ENU-based approach to generating an allelic series in any gene. *Mamm. Genome*, **15**, 585–591.
12. Schutte, B.C. and Murray, J.C. (1999) The many faces and factors of orofacial clefts. (Review). *Hum. Mol. Genet.*, **8**, 1853–1859.
13. Wilkie, O.M. and Morris-Kay, G.M. (2001) Genetics of craniofacial development and malformation. *Nat. Genet.*, **2**, 458–468.
14. Stanier, P. and Moore, G.E. (2004) Genetics of cleft lip and palate: syndromic genes contribute to the incidence of non-syndromic clefts. *Hum. Mol. Genet.*, **13**, R73–R81.
15. Tessier, P. (1976) Anatomical classification facial, cranio-facial and latero-facial clefts. *J. Maxillofac. Surg.*, **4**, 69–92.
16. Jin, J., Cardozo, T., Lovering, R.C., Elledge, S.J., Pagano, M. and Harper, J.W. (2004) Systematic analysis and nomenclature of mammalian F-box proteins. *Genes Dev.*, **18**, 2573–2580.
17. Skowyra, D., Craig, Tyers, K.L., Elledge, S.J. and Harper, J.W. (1997) F-box proteins are receptors that recruit phosphorylated substrates to the SCF ubiquitin–ligase complex. *Cell*, **91**, 209–219.
18. Feldman, R.M.R., Correll, C.C., Kaplan, K.B. and Deshaies, R.J. (1997) A complex of Cdc4p, Skp1p, and Cdc53p/cullin catalyzes ubiquitination of the phosphorylated CDK inhibitor Sic1p. *Cell*, **91**, 221–230.
19. Skowyra, D., Koepp, D.M., Kamura, T., Conrad, M.N., Conaway, R.C., Conaway, J.W., Elledge, S.J. and Harper, J.W. (1999) Reconstitution of G_1 cyclin ubiquitination with complexes containing SCF^{Grr1} and Rbx1. *Science*, **284**, 662–685.
20. Patton, E.E., Willems, A.R., Sa, D., Kuras, L., Thomas, D., Craig, K.L. and Tyers, M. (1998) Cdc53 is a scaffold protein for multiple Cdc34/Skp1/F-box protein complexes that regulate cell division and methionine biosynthesis in yeast. *Genes Dev.*, **12**, 692–705.
21. Kamura, T., Conrad, M.N., Yan, Q., Conaway, R.C. and Conaway, J.W. (1999) The Rbx1 subunit of SCF and VHL E3 ubiquitin ligase activates Rub1 modification of cullins Cdc53 and Cul2. *Genes Dev.*, **13**, 2928–2933.
22. Seol, J.H., Feldman, R.M., Zachariae, W., Shevchenko, A., Correll, C.C., Lyapina, S., Chi, Y., Galova, M., Claypool, J., Sandmeyer, S. *et al*. (1999) Cdc53/cullin and the essential Hrt1 RING-H2 subunit of SCF define a ubiquitin ligase module that activates the E2 enzyme Cdc34. *Genes Dev.*, **13**, 1614–1626.
23. Ohta, T., Michal, J.J., Schottelius, A.J. and Xiong, Y. (1999) ROC1, a homolog of APC11, represents a family of cullin partners with an associated ubiquitin ligase activity. *Mol. Cell*, **3**, 535–541.
24. Cardozo, T. and Pagano, M. (2004) The SCF ubiquitin ligase: insights into a molecular machine. *Nature*, **5**, 739–751.
25. Deshaies, R.J. (1999) SCF and cullin/RING H2-based ubiquitin ligases. *Annu. Rev. Cell Dev. Biol.*, **15**, 435–467.
26. Simon-Kayser, B., Scoul, C., Renaudin, K., Jezequel, P., Bouchot, O., Rigaud, J. and Bezieau, S. (2005) Molecular cloning and characterization of FBXO47, a novel gene containing an F-box domain, located in the 17q12 band deleted in papillary renal cell carcinoma. *Genes Chromosomes Cancer*, **43**, 83–94.
27. Le Poole, I.C., Sarangarajan, R., Zhao, Y., Stennett, L.S., Brown, T.L., Sheth, P., Miki, T. and Boissy, R.E. (2001) 'VIT1', a novel gene associated with vitiligo. *Pigment Cell Res.*, **14**, 475–484.
28. Cook, J., Lee, J.-H., yang, Z.-H., Krause, C., Herth, N., Hoffmann, R. and Pestka, S. (2006) FBXO11/PRMT9, a new protein arginine methyltransferase, symmetrically dimethylates arginine residues. *Biochem. Biophys. Res. Commun.*, **342**, 472–481.
29. Boisvert, F.-M., Côte, J., Boulanger, M.-C. and Richard, S. (2003) A proteomic Analysis of Arginine-methylated Proetin Complexes. *Mol. Cell Proteomics*, **2**, 1319–1330.
30. Li, D. (2003) Exploitation of host epithelial signaling networks by respiratory bacterial pathogens. *J. Pharmacol. Sci.*, **91**, 1–7.
31. Ravid, T. and Hochstrasser, M. (2004) NF-kB signaling: Flipping the switch with polyubiquitin chains. *Current Biology*, **14**, R898–R900.
32. Karin, M. and Ben-Neriah, Y. (2000) Phosphorylation meets ubiquitination: the control of NF-kB activity. *Ann. Rev. Immunol.*, **18**, 621–663.
33. Segade, F., Daly, K.A., Allred, D., Hicks, P.J., Cox, M., Brown, M., Hardisty-Hughes, R.E., Brown, S.D.M., Rich, S.S. and Bowden, D.W. (2006) Association of the FBO11 gene with COME/ROM in the Minnesota COME/ROM Family. *Arch. Otolaryngol. Head Neck Surg.* in press.
34. Nicklas, W., Baneaux, P., Boot, R., Decelle, T., Deeny, A.A., Fumanelli, M. and Illgen-Wilcke, B. (2002) Recommendations for health monitoring of rodent and rabbit colonies in breeding and experimental units. *Lab. Animals*, **36**, 20–42.